

Title: Light environment and seasonal variation in the visual system of the red shiner

2 (*Cyprinella lutrensis*)

4 Authors: Tarah N. Foster^{1,*}, Alyssa G. Williamson¹, Bradley R. Foster¹, and Matthew B.
Toomey^{1,*}

6

Affiliations: ¹Department of Biological Sciences, University of Tulsa, Oklahoma, 74104

8

*Corresponding authors: foster.tarah@gmail.com, matthew-toomey@utulsa.edu

10 **Abstract:** The light environment underwater can vary dramatically over space and time, challenging the visual systems of aquatic organisms. To meet these challenges, many
12 species shift their spectral sensitivities through changes in visual pigment chromophore and opsin expression. The red shiner (*Cyprinella lutrensis*) is a cyprinid minnow species
14 that has rapidly expanded its range throughout North America and inhabits a wide range of aquatic habitats. We hypothesized that visual system plasticity has contributed to the
16 red shiner's success. We investigated plasticity in chromophore usage and opsin expression by collecting red shiners from three Oklahoma creeks that vary in turbidity
18 throughout the year. We characterized the light environment by spectroradiometry, measured chromophore composition of the eyes with high performance liquid
20 chromatography, characterized CYP27C1 enzyme function through heterologous expression, and examined ocular gene expression by RNA sequencing and *de novo*
22 transcriptome assembly. We observed significantly higher proportions of the long-wavelength shifted A₂ chromophore in the eyes of fish from the turbid site and in
24 samples collected in winter, suggesting that there may be a temperature-dependent trade-off between chromophore-based spectral tuning and chromophore-related noise.
26 Opsin expression varied between turbid and clear creeks, but did not align with light environment as expected, and the magnitude of these differences was limited compared
28 to the differences in chromophore composition. We confirmed that red shiner CYP27C1 catalyzes the conversion of A₁ to A₂, but the ocular expression of CYP27C1 was not
30 well correlated with A₂ levels in the eye, suggesting conversion may be occurring outside of the eye.

Introduction

34 Many aquatic animals rely on vision, yet these organisms may face great
35 variation in their visual environment. The spectrum and intensity of light in the aquatic
36 environment varies with depth and is altered by the presence of sediments and
37 dissolved organic material (Cronin et al., 2014; Lythgoe, 1980; Lythgoe, 1988). There is
38 a wealth of evidence indicating that the spectral sensitivities of aquatic organisms have
39 evolved to match their specific light environment (Bowmaker et al., 1994; Margetts et
40 al., 2024) and the 'sensitivity hypothesis' predicts that this matching facilitates vision
41 (Lythgoe, 1980; Marshall et al., 2015). The strength of this relationship has made the
42 visual systems of fish an important model system for investigations linking molecular
43 change to ecological and evolutionary processes (Carleton et al., 2005; Fuller et al.,
44 2005; Rennison et al., 2016; Seehausen et al., 2008).

45 The aquatic light environment is dynamic with predictable (e.g. seasonal shifts in
46 productivity) and unpredictable (e.g. precipitation and turbidity) shifts in light intensity
47 and spectrum. Matching this dynamic light environment presents a special challenge
48 requiring plasticity within the visual system. The spectral sensitivities of fish are primarily
49 determined by the visual pigments of the photoreceptors that consist of the G-protein-
50 coupled receptor, opsin, and the vitamin A-derived molecule bound to it, the
51 chromophore (Carleton et al., 2020; Corbo, 2021). Spectral sensitivity can be fine-tuned
52 over the lifetime of an individual through: 1) changes in the type and level of opsin
53 expressed within a photoreceptor, and/or 2) changes to the chromophore component of
54 the visual pigment. Opsin expression has been extensively studied in multiple model
55 organisms demonstrating both environmentally induced plasticity and heritable genetic
56 determinants (Carleton, 2009; Fuller and Claricoates, 2011; Fuller et al., 2005; Härrer et
57 al., 2017; Hofmann et al., 2010; Karagic et al., 2018; Nandamuri et al., 2017; Rennison
58 et al., 2016; Veen et al., 2017). In contrast, the drivers and consequences of
59 chromophore plasticity are less well understood.

60 The chromophore component of the visual pigment absorbs photons of light and
61 isomerizes, causing a conformational change of the opsin that initiates the

62 phototransduction cascade, ultimately leading to light perception. Many freshwater fish
63 species use two different chromophore molecules, vitamin A₁-derived 11-*cis* retinal (A₁)
64 and vitamin A₂-derived 11-*cis* 3,4 didehydroretinal (A₂). The difference between the
65 vitamin A₁ and vitamin A₂ chromophores is an additional double bond within the terminal
66 β -ionone ring of A₂ (Corbo, 2021). When combined with many opsins, the additional
67 double bond in A₂ results in a long-wavelength shift in the sensitivity of the visual
68 pigment, relative to an A₁-containing pigment. The largest A₁ to A₂ shifts in sensitivity
69 are observed among longer-wavelength sensitive pigments (Corbo, 2021; Dartnall and
70 Lythgoe, 1965; Liebman and Entine, 1968; Munz and Schwanzara, 1967). Studies in
71 zebrafish (*Danio rerio*), have revealed that the enzyme cytochrome P450 27c1
72 (CYP27C1) mediates the conversion A₁ to A₂ within the retinal pigment epithelium of the
73 eye (Enright et al., 2015). CYP27C1-mediated chromophore switching is present in sea
74 lamprey (*Petromyzon marinus*) and likely widely conserved among vertebrates
(Morshedian et al., 2017).

75 Chromophore switching appears to be a widely expressed mechanism of visual
76 system plasticity, with shifts observed as animals migrate between different light
77 environments or as the environment changes with the seasons (Bridges, 1972; Corbo,
78 2021). For example, anadromous salmonids increase levels of vitamin A₂ chromophore
79 as adults migrate from the blue waters of the open ocean to the long-wavelength shifted
80 environments of their freshwater spawning sites (Alexander et al., 1994; Beatty, 1966).
81 Similarly, catadromous sea lamprey shift from A₂ to an A₁ chromophore as they migrate
82 from their natal freshwater streams and rivers to the relatively blue-shifted waters of
83 ocean spawning grounds (Crescitelli, 1956; Morshedian et al., 2017; Wald, 1957).
84 Among non-migratory freshwater fish species, increased levels of vitamin A₂
85 chromophore are associated with increased water turbidity (Bridges, 1964; Bridges,
86 1965; Bridges, 1972; Escobar-Camacho et al., 2019). These shifts in chromophore
87 composition are thought to be an adaptive plastic response that allow the animals to
88 match new or changed light environment.

89 The adaptive significance of seasonal shifts in chromophore composition are
90 more difficult to discern. Many freshwater fish species increase the A₂ chromophore
91 content of their eyes in the colder winter months, compared to the warmer summer

months (Bridges, 1964; Corbo, 2021; Temple et al., 2006; Whitmore and Bowmaker, 94 1989). It has been hypothesized that these seasonal shifts track a red-shift in the 96 aquatic light environments resulting from the positioning of the sun and abundance of 98 suspended particles (Bridges, 1972). However, there is less primary productivity in winter 100 and there may be less spectral filtering by plankton and algae which may result in a 102 relatively blue-shifted light environment. Therefore, it is difficult to predict how light 104 environment will change seasonally and it is likely to vary from site to site. Seasonal 106 changes in temperature may have a direct impact on chromophore function. Visual 108 pigments with the A₂ chromophore are less thermally stable than the A₁-containing 110 visual pigments (Ala-Laurila et al., 2007; Donner, 2020). Therefore, A₂-containing visual 112 pigments are more likely to isomerize and activate the phototransduction cascade in the 114 absence of light. Thus, it may be disadvantageous to utilize A₂ in warmer waters when 116 the probability of thermal isomerization is high. In cold waters, the probability of thermal 118 isomerization is lower, which may reduce the inherent noise associated with A₂ 120 chromophore. The extent to which red-shifted longer wavelength light environments 122 versus colder water temperatures induce shifts to a vitamin A₂-derived chromophore remains unresolved. Thus, chromophore composition plasticity may reflect a trade-off between signal-to-noise ratio of the photoreceptor response and spectral sensitivity that is dependent on both light environment and temperature.

112 In this study, we examined the associations between visual pigment 114 chromophore composition, light environment, and season in the red shiner (*Cyprinella* 116 *lutrensis*), a cyprinid minnow species native to the Mississippi river basin of North 118 America (Nico et al. 2019). The red shiner is an invasive species that has rapidly 120 expanded its range throughout North America (Mapping the potential distribution of the 122 invasive Red Shiner, *Cyprinella lutrensis* (Teleostei: Cyprinidae) across waterways of the conterminous United States). Red shiners thrive in waters varying widely in available light spectra, with mean of yearly median habitat turbidity measures ranging from 10 to 140 nephelometric turbidity units (NTU) and withstand temperatures ranging from 0°C-37°C (Dekar et al., 2014; Dugas and Franssen, 2012; Matthews, 1986; Matthews and Hill, 1977). Visual signaling is an important part of the biology of red shiners, with males displaying elaborate nuptial coloration (Dugas and Franssen, 2011).

124 This nuptial coloration is more intensely displayed in more turbid habitats (Dugas and
125 Franssen, 2011). The success of invasive red shiners may reflect their capacity for
126 phenotypical plasticity including in the visual system. Red shiners sampled from turbid
127 waters have relatively larger eyes, and fish reared in turbid conditions express higher
128 proportions of long-wavelength sensitive opsin (*LWS*) in their retinas (Chang and Yan,
129 2019; Dugas and Franssen, 2012). However, it is not known if red shiners also switch
130 chromophore composition or how this switch is influenced by the environmental
131 conditions this species encounters throughout the seasons. To address this question,
132 we sampled red shiners throughout the year from creeks with differing light
133 environments. We used high performance liquid chromatography to characterize the
134 chromophore composition of the retina and RNA sequencing to determine opsin
135 expression. We also characterized the enzymatic function of *CYP27C1* from the red
136 shiner utilizing a heterologous expression system.

Materials and Methods

138 *Field Sampling:* We sampled red shiners from Big Creek (36.785775, -95.469693),
139 Lightning Creek (36.655701, -95.464655), and Polecat Creek (36.017335, -95.985103)
140 in northeastern Oklahoma, USA from July 2020 to May 2022 (Fig. S1). These sites are
141 part of the Oklahoma Water Resources Board (OWRB) long-term monitoring efforts and
142 turbidity measures have been collected over multiple years. These measures indicate
143 that there are significant differences in turbidity among the sites and across the seasons
144 (site: $F_{2,77} = 5.60$, $P = 0.0054$, season: $F_{3,77} = 3.22$, $P = 0.027$, Fig. 1a, Fig. S1). Polecat
145 Creek was significantly more turbid than both Big Creek and Lightning Creek (Tukey
146 HSD, $P < 0.012$) and turbidity is significantly greater in spring compared to the winter
147 season (Tukey HSD, $P = 0.0032$). Fish were caught via minnow trap, dip net, or by
148 seining in accordance with method of take regulations set by the Oklahoma Department
149 of Wildlife Conservation under a scientific collector's permit (#10249373). Each site was
150 sampled 7 times during the study, and we collected a minimum of four and a maximum
151 of 28 individuals in each sampling bout. Fish were either euthanized on site or kept alive
152 in an aerated minnow bucket for no more than 1 hour and transported to the University
153 of Tulsa for subsequent euthanasia via overdose of Tricaine-S (MS222) and set on ice

154 (in either case). We immediately enucleated right and left eyes and transferred them to
155 a cooler containing dry ice (in the case of field dissection) or a -80° C freezer (in the
156 case of lab dissection). All samples were stored at -80° C until further analysis. All
157 methods were approved by the University of Tulsa Institutional Animal Care and Use
158 Committee (protocol number TU-0052). Eye diameter and standard body length were
159 measured post-mortem, to the nearest mm, with digital calipers. Fish sampled during
160 breeding season were sexed based on nuptial coloration and via dissection and
161 observation of testes or ovaries (Dugas and Franssen, 2011). Outside of the breeding
162 season, it was not possible to definitively determine sex from morphology.

Light Measurements: When possible, we collected downwelling irradiance measures at
164 the water's surface and at 20cm depth during each fish sampling bout. We used an
165 Ocean Optics Flame-S (serial #FLMS14357) miniature spectrometer coupled to an
166 Ocean Insight CC-3-UV-S- Cosine Corrector with Spectralon diffusing material for
167 irradiance measures. We calibrated the spectrophotometer with a radiometric calibrated
168 light source (HL-3P-CAL, Ocean optics Inc.) and initial measures were recorded in units
169 of irradiance ($\mu\text{Watt cm}^{-2}$). These data were processed in R (Team, 2021) utilizing
170 packages Pavo (Maia et al., 2019) and Tidyverse (Wickham et al., 2019). Irradiance
171 measures were converted to units of photon flux ($\mu\text{mol s}^{-1} \text{m}^{-2}$) and then summed from
172 300-700 nm to calculate total irradiance; percent transmission was calculated as the
173 total irradiance at 20 cm depth divided by the total irradiance at surface. Separately, to
174 assess variation in spectral composition we first normalized the transmission spectra
175 (integral equal to 1) to account for variations in brightness at different sites and dates.
176 This normalization allowed for our analysis to focus solely on variations in the light
177 spectrum due to absorbance in the water column. We adapted a measure from Wilwert
178 et al. (2021) and calculated the ratio of transmittance in the red (550-650 nm) vs. blue
179 portions (350-450 nm) of the spectrum (Fig. S1). All calculations were completed in R
180 (Team, 2021) utilizing packages Pavo (Maia et al., 2019) and Tidyverse (Wickham et
181 al., 2019).

182 *Retinoid Extraction and Analysis:* To determine the retinoid content of the red shiner
183 eyes, we used High Performance Liquid Chromatography (HPLC). Retinoids were

184 extracted from the whole right eye (left eye if right eye was not available) by grinding in
0.09% NaCl solution with 0.1 g of 2 mm zirconium beads (Next Advance, ZROB20) at
186 3000 hz for 90-120 seconds on a BeadBug Microtube Homogenizer (Model D1030).
This homogenization step was repeated two to three times for each sample. To
188 derivatize the retinaldehydes we then added 400 μ l of 2M hydroxylamine (Sigma,
255580) in distilled deionized water and 800 μ l of methanol and incubated for at least 10
190 minutes at room temperature in the dark (Kane and Napoli, 2010). We then added 800
 μ l of acetone and 1.75-2 ml of hexane for retinaldehyde extraction. Samples were
192 subsequently centrifuged for 3-5 minutes. The resulting solvent fraction was collected
and dried under a stream of nitrogen. We then resuspended the extract in 120 μ L of
194 hexane, and injected 100 μ L of sample into an Agilent 1100 series HPLC fitted with a
Zorbax RX-SIL column (4.6x25 mm, 5 μ m, Agilent). Elution of samples was achieved by
196 a gradient mobile phase of 0.5% ethyl acetate in hexane for 5 minutes then increased to
10% ethyl acetate in hexane for 20 minutes. Isocratic conditions for 35 minutes
198 followed. Throughout the run, the flow rate was 1.4 ml min⁻¹ and the temperature of the
column remained at 25°C. A photodiode array detector monitored the samples at 325,
200 350, and 380 nm. Authentic standards or published accounts were used to identify
vitamin A₁ and vitamin A₂-derived retinoids (Kane and Napoli, 2010; Landers and Olson,
202 1988; Moshedian et al., 2017; Zonta and Stancher, 1984). Retinoid mass was
calculated based on external standard curves for retinol and derivatized retinal. We
204 summed the mass of all A₁ or A₂-derived retinoids including retinols, retinaldehydes,
and retinyl esters and calculated the proportion of vitamin A₂-derived retinoid as the A₂
206 retinoid mass divided by total retinoid mass of the sample.

Statistics analyses of light environment and chromophore composition: We carried out
208 all statistical analyses in R (Team, 2021) using the base stats package except where
noted. We compared turbidity among the site and seasons by fitting the linear model:
210 $\text{Log}_{10}(\text{turbidity}) \sim \text{site} * \text{season}$ and tested the effects of the independent
variables with an ANOVA with type III sum of squares from using `car` package (Fox
212 and Weisberg, 2018). For post hoc pairwise comparisons we estimate marginal means
with the `emmeans` package (Lenth et al., 2019) and computed adjusted P-values by the

214 Tukey method. We follow the same approach to compare our direct measures of
215 spectral composition and a similar approach for light transmittance but fitted these
216 proportional measures to a beta-regression model with `betareg` package (Cribari-Neto
217 and Zeileis, 2010). To test for site and season effects on the relative abundance of A₂ in
218 the eyes of red shiners we fitted a beta-regression model: A₂ proportion ~ site
219 * season + eye diameter. A number of individuals had A₂ proportions = 0, which
220 violates the assumptions of beta-regression. Therefore, we transformed all of the
221 measures following the methods of (Cribari-Neto and Zeileis, 2010; Smithson and
222 Verkuilen, 2006). We included eye diameter in the model because it varied nearly 2-fold
223 among our samples and is an important determinant of the light gathering capacity of
224 the eye (Cronin et al., 2014). We did not include sex as an independent variable
225 because we were not able to determine the sex of all individuals we sampled. However,
226 we analyzed a subset of individuals sampled in summer when nuptial coloration and
227 gonad development allowed us to determine sex, and found that there were no
228 significant differences in A₂ abundance by sex ($F_{1,80} = 0.75, P = 0.39$) or the interaction
229 of sex and sampling site ($F_{2,80} = 0.12, P = 0.88$). We calculated post hoc contrasts with
230 `emmeans` as above and applied a Sidak adjustment (Lenth et al., 2019). Statistical
231 analysis of gene expression is detailed below.

232 *RNA Extraction and Transcriptome Analysis:* We extracted and purified total RNA from
233 the left eyes of 16 red shiner samples. We selected four individuals each from low
234 (Lightning creek) and high turbidity (Polecat creek) habitats in summer and late
235 fall/winter. Each eye was transferred to a screw-cap tube with 1 ml of TRIzol reagent
236 (ThermoFisher Scientific) and 0.1 g of 2 mm zirconium beads. We homogenized the
237 whole eyes with a BeadBug Microtube Homogenizer (Model D1030) at 4 kHz for 180
238 seconds. We then extracted RNA following the manufacturer's protocol with the addition
239 of 1 μ L of glycogen (R0551, Thermo Fisher Scientific) to facilitate RNA precipitation. To
240 remove residual DNA, we treated the extracted total RNA with Turbo DNase (AM1907,
241 ThermoFisher Scientific) following the manufacturer's guidelines. We extracted the
242 DNAse-treated RNA by adding 150 μ L molecular grade water and 200 μ L chloroform
243 and mixing the samples by vortexing. We then centrifuged the samples, collected the

244 aqueous fraction into a new tube, added 17.5 μ L NaAC (3M pH 5.2), 1 μ L glycogen,
245 and 600 μ L EtOH, and samples were incubated for 20 minutes at -20°C. Next, samples
246 were centrifuged at 13,000 rcf for 10 minutes at 4°C, and the resulting supernatant was
247 removed. Pellets were washed twice with 80% ethanol and air dried. Finally, the pellets
248 were resuspended with 25 μ L molecular grade water, and RNA quality and amount
were measured utilizing the NanoDrop 8000 (Thermo Scientific).

250 The total RNA samples were sent to the Clinical Genomics Laboratory at the
Oklahoma Medical Research Foundation (OMRF) for mRNA prep and sequencing.
252 mRNA sequencing libraries were prepared by OMRF with the xGen RNA Lib Prep Kit
(Integrated DNA Technologies) and NEB poly-A selection kit (New England Biolabs).
254 The mRNA libraries were then sequenced as 150 bp paired-end reads on an Illumina
NovaSeq 6000. We received demultiplexed reads in Fastq format and confirmed the
256 quality of the raw reads with FastQC (v0.11.5) (Andrews, 2015). We then removed
adaptor sequences and low-quality bases (Phred score <5) with Trim Galore! (v0.6.0)
258 (Krueger, 2019).

260 *De Novo Transcriptome Assembly:* A reference transcriptome was not available for *C.*
lutrensis; therefore, we generated a *de novo* transcriptome assembly with Trinity
(v2.8.4) (Grabherr et al., 2011) from the trimmed paired reads of two samples: a clear
262 water summer sample (LCV_7_24Jul20) and a turbid water late fall/winter sample
(PCJ_9_20Dec20). We supplemented the *de novo* assembly by referencing published
264 red shiner opsin gene sequences by Chang and Yan (2019) and the *CYP27C1*
sequence from this study. We used blastn (v2.13.0) (Camacho et al., 2009) to search
266 the *de novo* assembly against the published opsin sequences and the *CYP27C1*
sequence. We then merged the *de novo* and published sequences to create more
268 complete opsin and *CYP27C1* transcript sequences that included the 3' and 5'
untranslated regions (Table S1).

270 *Analyses of selected transcripts:* We pseudoaligned trimmed sequence reads in FastQ
format to the supplemented *de novo* transcriptome assembly (described above), and
272 generated read counts with Kallisto (v.0.46.2) using 50 bootstrap samples parameter -b

50 (Bray et al., 2016; Melsted et al., 2019) (Table S2). We exported the counts for all
274 genes as transcripts per million (TPM) using Sleuth (v.0.30.0) (Pimentel et al., 2017)
and then extracted the count data for the opsins and *CYP27C1* for further analysis. We
276 fitted separate linear models for each of the seven genes: $\text{Log}_2(\text{TPM}) \sim \text{site} * \text{season}$ and tested the effects of the independent variables with an ANOVA with type
278 III sum of squares, as described above. To account for multiple comparisons, we
adjusted the P-values with the `p.adjust` function of base R and applied a Benjamini &
280 Hochberg correction for seven comparisons. We also calculated the expression of each
opsin as a proportion of total opsin expression of all six opsins in each sample and fitted
282 a beta-regression model, tested with an ANOVA with type III sum of squares, and
adjusted P-values as described above.

284

Cloning and Functional Characterization of CYP27C1: To examine the catalytic
286 function of CYP27C1 in the red shiner, we extracted RNA from the left eye of an adult
female as described above. We generated cDNA by reverse transcription using an oligo
288 (dT) 20 primer and superscript IV reverse transcriptase (18090010, ThermoFisher
Scientific) following the manufacturer's protocols. We amplified the full-length coding
290 sequence of CYP27C1 by polymerase chain reaction with the forward primer:
ataccgcaccggtagccaccATGGCTCTCAAAGTACTATTCTACACATGG and reverse
292 primer: ataccgcgcggccgcTTTCGGTCTGTAAATCTAAGGTTGATGG. The lower-case
sequence is additional sequence which contains the restriction sites for cloning. We
294 digested the PCR products with *Age*I and *Not*I (New England Biolabs) and cloned them
into the first position of the bicistronic vector pCAG-[first position]-2A-GFP. We
296 confirmed the CYP27C1 sequence with Sanger sequencing (Eurofins Genomics). We
assayed enzymatic activity in HEK293 cells (ATCC, CRL-1573). Following the ATCC
298 protocols, we cultured the cells to 80% confluence in a 6-well plate (8.96 cm² wells) and
then transfected with the CYP27C1 construct or a control construct (pCAG-dsRed-2A-
300 GFP) using polyethylenimine (PEI, 23966-2, Polysciences, Warrington, PA). After 24
hours, we confirmed expression by visualizing GFP. We then dissolved 5 µg of retinol
302 (Sigma, R7632) in 36 µl of ethanol and combined with 6 ml of complete media. We
replaced the media in the wells with 1 mL each of the retinol-enriched media and

304 incubated overnight (~24 hrs). We then scraped the cells, discarded the media, and
305 extracted carotenoids by adding 200 μ l of distilled water, 200 μ l of 100% ethanol, and
306 disrupted the cells with 0.1g of 1 mm zirconium beads (Next Advance, ZROB10) at 4
307 kHz for 30 seconds on a Beadbug homogenizer. We then added 1 ml of hexane:tert-
308 butyl methyl ether (1:1, vol:vol), homogenized again for 30 seconds, then centrifuged at
309 10,000 RPM for two minutes. We collected the upper solvent fraction from the sample
310 and dried the extract under a stream of nitrogen. We then redissolved the cell extracts
311 in 120 μ l of hexane and analyzed retinoid content by HPLC, as described above.

312

Results

314 *Light environment differs among study sites:*

We measured downward irradiance at 20 cm depth at each site and most
315 sampling bouts and determined the transmittance relative to surface illumination and
316 spectral composition. Light transmittance differed significantly among the sites by
317 season (site*season: $F_{6,87} = 13.008$, $P = 1.90 \times 10^{-10}$, Fig. 1c). Post hoc analyses
318 indicated that Big Creek had significantly greater transmittance than the other sites, in
319 spring (Sidak adjusted comparisons $P < 0.0022$, Fig 1c). In summer, all three sites
320 differed significantly (Sidak adjusted comparisons $P < 0.0031$) with the greatest
321 transmittance at Lightning creek and lowest at Polecat creek (Fig. 1c). In the fall, Big
322 Creek and Lightning Creek did not differ significantly, however, both had significantly
323 greater transmittance than Polecat Creek (Sidak adjusted comparisons $P < 0.0001$, Fig
324 1c). In winter, only Big Creek and Polecat Creek differed significantly (Sidak adjusted
325 comparisons $P = 0.014$, Fig 1c). Consistent with the historical turbidity measures (Fig.
326 1b), Lightning Creek tended to have the greatest transmittance (i.e. clearest waters),
327 Big Creek was intermediate to the two other sites, and Polecat Creek had the lowest
328 transmittance of all three sites. A notable exception to this trend was during spring,
329 when we observed very low transmittance in Lightning Creek following heavy rainfall.

The spectral composition of the light environment differed significantly among
330 sites by season (site*season: $F_{6,88} = 39.592$, $P = 2.20 \times 10^{-16}$, Fig. 1d). Post hoc

comparisons indicate that the red to blue ratio differed significantly between Big Creek
334 and Lightning Creek only during spring (Sidak adjusted comparison $P < 0.0001$).

However, during all seasons, the spectrum at Polecat Creek was significantly redder
336 than the other sites (Sidak adjusted comparisons $P < 0.0001$, Fig. 1d). At Lightning
338 Creek and Polecat Creek the spectrum was significantly redder in spring compared to
other seasons (Sidak adjusted comparisons $P < 0.0001$, Fig. 1d). At Polecat Creek the
340 spectrum was significantly blue shifted in the fall compared to all other seasons (Sidak
adjusted comparisons $P < 0.0001$, Fig. 1d).

Red Shiner Ocular Retinoid Composition: Our initial HPLC profiling confirmed that the
342 red shiner is a dual visual pigment species. We observed both A₁ and A₂ retinyl esters,
aldehydes, and alcohols (Fig. S3) in the eyes of many of the individuals we sampled.
344 Retinal aldehydes were the most abundant of these forms in the eye (Fig. S3). Next, we
investigated how retinoid composition varied among populations from different sites and
346 seasons.

A₂-Derived Chromophore varies among sites and seasons:

348 To understand if and how visual pigment chromophore composition varied, we
sampled fish from different locations throughout the year and measured the retinoid
350 content by HPLC. We found that the proportion of A₂-derived chromophore differed
significantly among sites by season (site * season: $F_{6,202} = 3.0511$, $P = 0.0070$, Fig.
352 2a). In all seasons, fish sampled from Polecat Creek, the most turbid site, had a
significantly greater proportion of A₂ chromophore than the other two sites (Sidak
354 adjusted comparisons $P < 0.0077$, Fig. 2a). At each site, the proportion of A₂
chromophore in the eyes of the fish differed significantly among the seasons with
356 significantly lower proportions in summer compared to the winter samples (Sidak
adjusted comparisons $P < 0.0002$, Fig. 2a). Eye size was also a significant predictor of
358 A₂ chromophore abundance ($F_{1,202} = 5.7146$, $P = 0.018$) and fish with larger eyes
tended to accumulate a greater proportion of A₂ chromophore (Fig. 2b)

360 *CYP27C1 from Cyprinella lutrensis Catalyzes the Conversion of Retinol to 3,4-
didehydroretinol:*

362 The enzyme CYP27C1 catalyzes the conversion of retinol to 3,4-didehydroretinol
363 in zebrafish and evidence suggests that this mechanism is widely conserved among
364 vertebrates (Enright et al., 2015; Morshedian et al., 2017). To confirm that the red shiner
365 homolog of CYP27C1 possesses this same catalytic function, We cloned *C. lutrensis*
366 CYP27C1, heterologously expressed the enzyme, and assayed its activity with a retinol
367 substrate. The amino acid sequences of red shiner CYP27C1 is similar to the zebrafish
368 homolog with 488/540 (90%) amino acid identities (Fig. S4). HEK293 cells expressing
369 red shiner CYP27C1 and supplemented with retinol produced a novel product that has a
370 red-shifted UV-Vis absorbance spectrum and HPLC retention times consistent with 3,4-
371 didehydroretinol (Fig. 3).

372 *Opsin and CYP27C1 gene expression patterns:*

373 Previous studies have demonstrated adaptive plasticity in opsin expression is
374 linked to light environment and that CYP27C1 is the enzyme that catalyzes the
375 conversion of A₁ to A₂ derived chromophore (Carleton et al., 2020; Chang and Yan,
376 2019; Corbo, 2021). Therefore, we wanted to know if and how the expression of these
377 genes varied in the eyes of red shiners sampled from our study sites. To do this, we
378 sequenced the ocular transcriptomes of a subset of individuals from the most (Polecat
379 Creek) and least (Lightning Creek) turbid sites in summer and fall/winter seasons. We
380 sequenced the transcriptomes to an average depth of 24,114,599 reads per sample
381 with an average of 52.23 percent alignment with our *de novo* transcriptome assembly
382 (Table S2).

383 In contrast to the dramatic differences in A₂ chromophore abundance among
384 sites and across seasons (Fig. 2a), we did not observe significant differences in
385 CYP27C1 expression among our subset of samples (site: $F_{1,12} = 4.00$, $P_{adj} = 0.16$,
386 season: $F_{1,12} = 0.28$, $P_{adj} = 1.00$, Fig. 4a). CYP27C1 expression ranged from 0 to 9.2
387 TPM among the samples, a level of expression that is generally considered “low”
388 (Papatheodorou et al., 2018).

389 We compared the expression of the opsins two different ways. First, we directly
390 compared the normalized transcript counts of each opsin (transcripts per million – TPM)

and then, to capture possible opsin-based shifts in spectral sensitivity, we calculated the
392 proportional expression of each opsin relative to the total opsin expression in the
sample. *Rhodopsin 1 (RH1)* was the most highly expressed opsin in all samples (Fig 4)
394 and the normalized and relative expression of *RH1* differed significantly between sites
by season (TPM ~ site * season: $F_{1,12} = 9.45$, $P_{adj} = 0.023$, proportion ~ site
396 * season: $F_{1,11} = 18.37$, $P_{adj} = 0.003$). The relative expression of *RH1* in the Lightning
Creek (low turbidity site) sample was significantly greater than the Polecat Creek (high
398 turbidity site) samples in the summer season (Sidak adjusted comparisons $P < 0.0001$,
Fig. 4b), and relative *RHO* expression in the Polecat Creek samples significantly
400 increased from summer to the late fall/winter samples (Sidak adjusted comparisons $P <$
 0.0001 , Fig. 4b).

402 *Long wavelength-sensitive opsin 1 (LWS1)* normalized expression was
significantly greater in the Lightning Creek samples (site: $F_{1,12} = 13.51$, $P_{adj} = 0.011$), but
404 there were no significant differences between sites or seasons in *LWS1* relative
expression (Fig. 4b).

406 Like many other teleost fish, the medium wavelength sensitive *rhodopsin 2 (RH2)*
has been duplicated, and two forms, RH2a and RH2b, are present in the red shiner
408 genome (Chang and Yan, 2019; Musilova and Cortesi, 2023). The normalized
expression of the *RH2a* differed significantly between seasons with higher levels
410 observed in the summer samples (season: $F_{1,12} = 13.54$, $P_{adj} = 0.011$, Fig. 4a). The
relative expression of *RH2a* differed significantly among sites (site: $F_{1,11} = 36.53$, P_{adj}
412 = 0.00029) with levels significantly higher in the Polecat Creek (high turbidity) samples
in the summer (Sidak adjusted comparisons $P < 0.0001$) and declining significantly from
414 summer to late fall/winter (Sidak adjusted comparisons $P < 0.0001$). The normalized
expression of *RH2b* was significantly greater in the Lightning Creek samples (site:
416 $F_{1,12} = 31.00$, $P_{adj} = 0.0004$), but there were no significant differences in relative
expression of *RH2b* between sites or seasons (Fig. 4b).

418 The normalized expression of the *short wavelength-sensitive opsins 1 and 2*
(*SWS1* and *SWS2*) differed significantly between the sites by season (*SWS1* site *
420

420 season: $F_{1,12} = 6.81$, $P_{adj} = 0.053$, SWS2 site * season: $F_{1,12} = 11.34$, $P_{adj} = 0.013$,
Fig. 4a). The normalized expression of SWS1 and SWS2 was significantly greater in
422 Lightning Creek (low turbidity site) samples in the summer (Sidak adjusted comparisons
 $P < 0.0064$, Fig. 4a) and SWS2 levels in Lightning Creek samples decline significantly
424 from summer to late fall/winter (Sidak adjusted comparison $P < 0.035$, Fig. 4a). There
were no significant differences in SWS1 or SWS2 relative expression between sites or
426 seasons (Fig. 4b).

Discussion

428 Our results show that the red shiner is a dual chromophore species with a plastic
visual system where the relative abundance of the A₁ and A₂ visual pigment
430 chromophores differed significantly among habitats and seasons. We demonstrate that
red shiner CYP27C1 catalyzes the conversion of vitamin A₁-derived chromophore to
432 vitamin A₂-derived chromophore, but the expression patterns of CYP27C1 in the eye
are not consistent with the patterns of A₂ chromophore abundance. We observed
434 significant variation in visual pigment opsin expression among habitats and seasons,
but this variation was not consistent with patterns of environmental variation reported in
436 other teleost fish.

438 *Chromophore composition matches median light environment and shifts with the
seasons.*

We predicted that red shiners inhabiting turbid waters would have a higher
440 proportion of A₂ chromophore in their eyes than those inhabiting less turbid water.
Consistent with this prediction, we found the proportion of A₂ chromophore to be
442 significantly greater in fish from the historically most turbid site, Polecat Creek,
compared to the sites with clearer waters, Lightning Creek and Big Creek. This pattern
444 of turbidity-dependent chromophore composition is consistent with studies of the golden
shiner (*Notemigonus crysoleucas*) and a variety of cichlid species that show greater
446 proportions of A₂ chromophore in the eyes or photoreceptors of individuals sampled
from turbid habitats (Bridges, 1964; Carleton and Yourick, 2020; Escobar-Camacho et
448 al., 2019; Härrer et al., 2018; Terai et al., 2017). These habitat-specific patterns of

chromophore composition are considered adaptive, and it is hypothesized that the a
450 shift from an A₁ to A₂ chromophore dominated retina will red-shift visual sensitivity to
match the red-shifted light environment of turbid waters (Bridges, 1964; Bridges, 1972;
452 Corbo, 2021; Enright et al., 2015; Escobar-Camacho et al., 2019). Consistent with this
hypothesis, our measures confirmed that the available light spectrum in the most turbid
454 site, Polecat Creek, was significantly red shifted compared to the clearer water sites.

The light environments at our study sites were dynamic, and we observed
456 considerable variation within seasons and significant changes across the seasons.
Laboratory investigations of the A₁ to A₂ chromophore switch in zebra fish (*Danio rerio*)
458 indicate that these changes occur over the course of weeks (Enright et al., 2015).
Therefore, short-term changes in light environment, like the influx of turbid water
460 following a single thunderstorm, are unlikely to be closely tracked by changes in
chromophore composition. To test this prediction, we refit our model predicting A₂
462 chromophore with our direct measures instead of site as a factor, compared the fits of
these models by AICc, and found that these models were poorer fits (Δ AICc > 102)
464 than the “site” model (Table S3). This result suggests that the mechanisms of
chromophore plasticity may be integrating over a longer-time scale and tuning the visual
466 system to the mean or median conditions in a habitat.

We observed seasonal changes in chromophore composition, but our results
468 suggest that these are not strongly linked to the light environment. Historical turbidity
measures indicate that turbidity tends to be lower in the winter months and peaks during
470 the rainy late spring and early summer season. Our direct measures of light
environment are partially consistent with this trend, with some of the sights showing
472 increased transmittance and a relative blue shift in the spectrum. Therefore, if red
shiners are matching their visual sensitivities to these seasonal changes in the light
474 environment, we expect a shift from the A₂ chromophore to the relatively blue-shifted A₁
chromophore during the winter months. However, this prediction was not supported, as
476 the proportion of the A₁-derived chromophore decreased in the winter months in the
eyes of red shiners at all sites. This suggests that chromophore composition is
478 responding to something other than the spectral composition of light.

A shift toward increased A₂ chromophore levels in the winter months has been
480 observed in a diversity of fish species and also an amphibian (Bridges, 1964; Bridges,
1965; Bridges, 1972; Makino et al., 1983; Muntz and Mouat, 1984; Ueno et al., 2005).
482 Detailed experimental investigations in the 1970's and 80's identified temperature and
light as important drivers of chromophore composition. The effects of experimental light
484 manipulations are complex. Total darkness, occlusion of the eye, or reduced daylight
hours consistently favor a shift to and A₂ chromophore dominance (Allen, 1971; Allen
486 and McFarland, 1973; Bridges and Yoshikami, 1970; Tsin and Beatty, 1977), but there
is also evidence that high light intensity leads to increases in A₂ chromophore levels
488 (Allen, 1971; Cristy, 1976). In contrast, across all studies, low temperatures consistently
resulted in a shift from A₁ to A₂ as the dominant chromophore in the eye (Allen and
490 McFarland, 1973; Cristy, 1976; McFarland and Allen, 1977; Tsin and Beatty, 1977).

Seasonal and temperature driven shifts in chromophore composition may reflect
492 an adaptive balance of spectral tuning and photoreceptor noise. A₂ containing visual
pigments are more susceptible, than A₁ visual pigments, to spontaneous isomerization
494 in the absence of light (Ala-Laurila et al., 2007). Therefore, the shift from an A₁ to A₂
chromophore increases dark noise within the cell and reduces the sensitivity of the
496 photoreceptor (Ala-Laurila et al., 2007; Barlow, 1956). A₂ containing visual pigment
instability is positively temperature-dependent however, and this dark noise is predicted
498 to be less at lower temperatures (Aho et al., 1988). Therefore, the cost (loss of visual
sensitivity) may be reduced in cold conditions as red shiners are able to utilize A₂
500 chromophore and expand the light spectrum that is visible without the cost of
spontaneous isomerization. Despite these seasonal shifts, chromophore differences
502 among the study sites remain, suggesting the regulation of chromophore composition is
finely tuned and likely integrates several environmental cues. Thus, the red shiner offers
504 an excellent opportunity to deconstruct these mechanisms of regulation and a readily
accessible natural system to investigate how local environments drive the evolution of
506 this plasticity.

CYP27C1 expression patterns are inconsistent with chromophore composition.

508 The enzyme CYP27C1 has been identified as necessary and sufficient to
catalyze the conversion of vitamin A₁ to vitamin A₂ in zebrafish (Enright et al., 2015).
510 Subsequent studies suggest that this mechanism of chromophore metabolism is widely
conserved among vertebrates (Morshedian et al., 2017). Consistent with this conserved
512 function, we found that red shiner CYP27C1 was sufficient to convert retinol (A₁) to 3,4-
didehydroretinol (A₂) in our cell culture assay system. Therefore, we hypothesized that
514 changes in *CYP27C1* expression were mediating the environmental and seasonal
variation and predicted that *CYP27C1* expression levels in the eyes of red shiners
516 would track A₂ chromophore abundance. However, this prediction was not supported by
our transcriptome profiling analyses of whole eyes. We found that *CYP27C1* expression
518 was low in all samples and there were no significant differences in expression among
sites or seasons. However, this result does not rule out a role for CYP27C1 in
520 chromophore conversion. We extracted RNA from whole eyes, therefore our ability to
detect changes in *CYP27C1* may have been confounded by the complex collection of
522 tissues and cell types in the samples. Enright et al. (2015) found that CYP27C1
expression concentrated in the retinal pigment epithelium of the eye, and a targeted
524 analysis of these cells may reveal a different pattern. Vitamin A₂ has been found to be
the dominant retinoid form in the plasma and liver tissues of several fish species,
526 suggesting that the conversion of vitamin A₁ to vitamin A₂ might be occurring outside of
the eye (Balasundaram et al., 1956; Defo et al., 2012; Goswami and Barua, 1981). An
528 investigation of the distribution of A₁ and A₂ dynamics in other tissues of the red shiner
is warranted.

530 The ocular expression of *CYP27C1* has been used as a proxy measure for
chromophore composition in several recent studies (Karagic et al., 2022; Wilwert et al.,
532 2022; Wilwert et al., 2023). However, in our study, patterns of chromophore abundance
and ocular expression of *CYP27C1* were not concordant. A similar discordance was
534 observed by Escobar-Camacho et al. (2019) where they found that ocular *CYP27C1*
expression was significantly lower among turbid habitat fish with higher A₂ levels. These
536 results indicate that the assumed correlation between ocular *CYP27C1* levels and
chromophore composition should be validated within each study system.

538 *Opsin expression varied among habitats and seasons.*

Chang and Yan (2019), in a laboratory study, demonstrated that opsin expression is plastic and that red shiners increase *LWS* opsin, and decrease *SWS* opsin expression in turbid, red-shifted light environments (Chang and Yan 2019). Therefore, we predicted that the red shiners we sampled from turbid environments would show a similar pattern of elevated *LWS* and reduced *SWS* opsin expression compared to those sampled from clearer water conditions. Contrary to this prediction, we found no significant differences in the relative expression of *LWS1*, *RH2b*, *SWS1*, or *SWS2* between the site or seasons. There are several reasons why our results might differ from Chang and Yan (2019). While the fish in the previous study were purchased from aquarium suppliers and reared under captive conditions, we studied wild-caught fish. The artificial light environments of the captive study may differ considerably from the habitats we sampled. The lowest turbidity environment in the lab study was 0 NTU, and the significant variance in *LWS* expression was found only between 0 NTU and each higher turbidity environment (50, 100 and 200 NTU) (Chang and Yan, 2019). The median turbidity at our clear water site was 3.0 NTU, and the turbid site 20.4 NTU. Perhaps the most turbid lightning environment (Polecat Creek) in our study was not challenging enough to elicit significant variation in opsin expression.

556 The only cone opsin that differed in its relative expression was the medium wavelength sensitive *RH2a* with relatively high expression among fish sampled in the 558 most turbid conditions (summer, Polecat creek). Diverging response in the expression 560 of the *RH2a* and *RH2b* opsin paralogs have also been observed among guppies (*Poecilia reticulata*), raising the interesting possibility that these opsins may be sub-functionalized in a yet unknown way (Ehlman et al., 2015; Musilova and Cortesi, 2023).

562 The relative expression of rod opsin *RH1* was significantly higher among fish from the clear water sites, and its expression among the turbid-site fish increased from 564 summer to the fall/winter season. This suggested that the relative expression of *RH1* 566 may be influenced by water clarity and positively correlated with available light levels. Among Lake Tanganyika cichlid species, *RH1* expression is positively correlated with 568 eye size, an important determinant of the amount of light reaching the photoreceptors (Ricci et al., 2023). Rod photoreceptors mediate scotopic vision, therefore the shifts we

see in the relative expression of *RH1* might reflect or impact diel activity patterns of red
570 shiners in different habitats. In other words, are fish in clear water sites more active in
low light conditions?

572 When we examined opsin transcript levels (TPM values), rather than expression
relative to the other opsins, we found that the expression of most of the opsins was
574 significantly higher in samples from the clear water site, especially in the summer
season. This finding is contrary to previous studies findings where increased expression
576 of cone opsins was observed in turbid conditions compared to clear water conditions
(Chang and Yan, 2019; Fuller and Claricoates, 2011). The transcript level variations we
578 observed are consistent with light levels and day-length driving opsin expression in
general. For example, daily rhythms of opsin expression have been identified in the
580 Senegalese sole and a species of African cichlid (Frau et al., 2020; Halstenberg et al.,
2005). Sole kept under alternating light and dark conditions, with either white or blue
582 light spectra, had peak opsin expression at the end of the light period or at the second
half of the day (Frau et al., 2020). Similarly, Halstenberg et al. (2005) found all cone
584 opsins analyzed peaked in expression during the late afternoon in the African cichlid,
Haplochromis burtoni. Therefore, long days in the summer months and clear water
586 conditions may promote opsin expression in general.

Conclusions

588 The red shiner's abundance, wide distribution in North America, and dual pigment visual
system make it an excellent model organism for visual system plasticity research. We
590 have demonstrated significant variation in visual pigment chromophore composition
relative to light environment, and season suggesting this is a plastic trait. These
592 variations in chromophore composition are likely to have a substantial impact on the
sensitivities and function of the red shiner visual system and highlight the importance of
594 considering the A₁ to A₂ chromophore switch as an integral part of visual system
plasticity. The significant relationship between chromophore composition and season
596 suggests there may be a trade-off between spectral tuning and receptor noise
thresholds, presenting an exciting opportunity to understand how multiple environmental
598 cues are integrated to shape plastic responses. Opsin expression has historically been

the focus of visual system plasticity research. However, our results indicate that habitat
600 and season related variation in chromophore composition is greater than variation in
opsin expression. Therefore, in red shiners, and possibly other fish species,
602 chromophore composition may be a more important mechanism of visual system
plasticity.

604 **Acknowledgments**

We thank Matthew Dugas for his advice on red shiner sampling, study site selection, and
606 study design. We thank Ronald Bonnet and Alexandra Kingston for their contributions to study
design, analysis, and interpretation. We thank Dustin Smith and Desirae Gonzales for their
608 assistance in the field. We are grateful to Lance Phillips at the Oklahoma Water Resources
Board and Karla Spinner at The Oklahoma Conservation Commission for providing access to
610 historical turbidity records. The computing for this project was performed at the OU
Supercomputing Center for Education & Research (OSCER) at the University of Oklahoma
612 (OU).

Author contributions

614 Conceptualization: T.F., M.T.; Methodology: T.F., B.F., M.T.; Formal analysis: T.F., A.W., B.F.,
M.T.; Investigation: T.F., A.W., B.F., M.T.; Resources: M.T.; Writing - original draft: T.F., M.T.;
616 Writing - review & editing: T.F., A.W., B.F., M.T.; Visualization: T.F., M.T.; Supervision: T.F.,
M.T.; Funding acquisition: M.T.

618 **Funding:**

T. F. was partially supported by funds from the Mervin Bovaird endowment. This work was
620 supported by startup funds from the University of Tulsa and the National Science Foundation
(IOS 2037739).

622 **Data availability:**

624 RNA sequencing data have been deposited with the NCBI short-read archive (BioProject ID:
PRJNA1076457). The transcriptome assembly and other raw data files and analysis scripts
626 are available in the Dryad Digital Repository - <https://doi.org/10.5061/dryad.vhhmgqp2c> -
temporary reviewer link - <https://datadryad.org/stash/share/J8mL6UfTw-gS0AUsljiN9UMw7nSYbMYkLKs0U7MbGQ>.

628 **References:**

630 **Aho, A. C., Donner, K., Hydén, C., Larsen, L. O. and Reuter, T.** (1988). Low retinal noise in animals with low body temperature allows high visual sensitivity. *Nature* **334**, 348–350.

632 **Ala-Laurila, P., Donner, K., Crouch, R. K. and Cornwall, M. C.** (2007). Chromophore switch from 11-cis-dehydroretinal (A_2) to 11-cis-retinal (A_1) decreases dark noise in salamander red rods. *J. Physiol.* **585**, 57–74.

634 **Alexander, G., Sweeting, R. and McKeown, B.** (1994). The shift in visual pigment dominance in the retinae of juvenile coho salmon (*Oncorhynchus kisutch*): an indicator of smolt status. *J. Exp. Biol.* **195**, 185–197.

638 **Allen, D. M.** (1971). Photic control of the proportions of two visual pigments in a fish. *Vision Res.* **11**, 1077–1112.

640 **Allen, D. M. and McFarland, W. N.** (1973). The effect of temperature on rhodopsin-porphyrin ratios in a fish. *Vision Res.* **13**, 1303–1309.

642 **Andrews, S.** (2015). *FastQC: A Quality Control Tool for High Throughput Sequence Data [Online]*.

644 **Balasundaram, S., Cama, H. R., Sundaresan, P. R. and Varma, T. N.** (1956). Vitamin A_2 in Indian fresh-water fish-liver oils. *Biochem. J.* **64**, 150–154.

646 **Barlow, H. B.** (1956). Retinal noise and absolute threshold. *J. Opt. Soc. Am.* **46**, 634–639.

648 **Beatty, D. D.** (1966). A study of the succession of visual pigments in pacific salmon (*Oncorhynchus*). *Can. J. Zool.* **44**, 429–455.

650 **Bowmaker, J. K., Govardovskii, V. I., Shukolyukov, S. A., Zueva, L. V., Hunt, D. M., Sideleva, V. G. and Smirnova, O. G.** (1994). Visual pigments and the photic environment: the cottoid fish of Lake Baikal. *Vision Res.* **34**, 591–605.

652 **Bray, N. L., Pimentel, H., Melsted, P. and Pachter, L.** (2016). Near-optimal probabilistic RNA-seq quantification. *Nat. Biotechnol.* **34**, 525–527.

654 **Bridges, C. D.** (1964). Effect of season and environment on the retinal pigments of two fishes. *Nature* **203**, 191–192.

656 **Bridges, C. D. B.** (1965). Visual Pigments in a Fish exposed to Different Light-Environments. *Nature* **206**, 1161–1162.

658 **Bridges, C. D. B.** (1972). The rhodopsin-porphyrin visual system. In *Handbook of Sensory Physiology VII* (ed. Dartnall, H. J. A.), pp. 417–480. Berlin: Springer.

660 **Bridges, C. D. and Yoshikami, S.** (1970). The rhodopsin-porphyrin system in freshwater fishes. 1. Effects of age and photic environment. *Vision Res.* **10**, 1315–1332.

662 **Camacho, C., Coulouris, G., Avagyan, V., Ma, N., Papadopoulos, J., Bealer, K. and Madden, T. L.** (2009). BLAST+: architecture and applications. *BMC Bioinformatics* **10**, 421.

664 **Carleton, K.** (2009). Cichlid fish visual systems: mechanisms of spectral tuning. *Integr. Zool.* **4**, 75–86.

666 **Carleton, K. L. and Yourick, M. R.** (2020). Axes of visual adaptation in the ecologically diverse family *Cichlidae*. *Semin. Cell Dev. Biol.* **106**, 43–52.

668 **Carleton, K. L., Parry, J. W., Bowmaker, J. K., Hunt, D. M. and Seehausen, O.** (2005). Colour vision and speciation in Lake Victoria cichlids of the genus *Pundamilia*. *Mol. Ecol.* **14**, 4341–4353.

672 **Carleton, K. L., Escobar-Camacho, D., Stieb, S. M., Cortesi, F. and Marshall, N. J.** (2020). Seeing the rainbow: mechanisms underlying spectral sensitivity in teleost fishes. *J. Exp. Biol.* **223**.

674 **Chang, C.-H. and Yan, H. Y.** (2019). Plasticity of opsin gene expression in the adult red shiner (*Cyprinella lutrensis*) in response to turbid habitats. *PLoS One* **14**, e0215376.

676 **Corbo, J. C.** (2021). Vitamin A1/A2 chromophore exchange: its role in spectral tuning and visual plasticity. *Dev. Biol.*

678 **Crescitelli, F.** (1956). The nature of the lamprey visual pigment. *J. Gen. Physiol.* **39**, 423–435.

Cribari-Neto, F. and Zeileis, A. (2010). Beta Regression in R. *J. Stat. Softw.* **34**, 1–24.

680 **Cristy, M.** (1976). Effects of temperature and light intensity on the visual pigments of rainbow trout. *Vision Res.* **16**, 1225–1228.

682 **Cronin, T. W., Johnsen, S., Justin Marshall, N. and Warrant, E. J.** (2014). *Visual Ecology*. Princeton University Press.

684 **Dartnall, H. J. and Lythgoe, J. N.** (1965). The spectral clustering of visual pigments. *Vision Res.* **5**, 81–100.

686 **Defo, M. A., Pierron, F., Spear, P. A., Bernatchez, L., Campbell, P. G. C. and Couture, P.** (2012). Evidence for metabolic imbalance of vitamin A₂ in wild fish chronically exposed to metals. *Ecotoxicol. Environ. Saf.* **85**, 88–95.

690 **Dekar, M. P., McCauley, C., Ray, J. W. and King, R. S.** (2014). Thermal Tolerance, Survival, and Recruitment of Cyprinids Exposed to Competition and Chronic Heat Stress in Experimental Streams. *Trans. Am. Fish. Soc.* **143**, 1028–1036.

692 **Donner, K.** (2020). Spectral and thermal properties of rhodopsins: closely related but not tightly coupled.

694 **Dugas, M. B. and Franssen, N. R.** (2011). Nuptial coloration of red shiners (*Cyprinella lutrensis*) is more intense in turbid habitats. *Naturwissenschaften* **98**, 247–251.

696 **Dugas, M. B. and Franssen, N. R.** (2012). Red shiners (*Cyprinella lutrensis*) have larger eyes in turbid habitats. *Can. J. Zool.* **90**, 1431–1436.

698 **Ehlman, S. M., Sandkam, B. A., Breden, F. and Sih, A.** (2015). Developmental plasticity in vision and behavior may help guppies overcome increased turbidity. *J. Comp. Physiol. A Neuroethol. Sens. Neural Behav. Physiol.* **201**, 1125–1135.

700

702 **Enright, J. M., Toomey, M. B., Sato, S.-Y., Temple, S. E., Allen, J. R., Fujiwara, R., Kramlinger, V. M., Nagy, L. D., Johnson, K. M., Xiao, Y., et al.** (2015). Cyp27c1 Red-Shifts the Spectral Sensitivity of Photoreceptors by Converting Vitamin A₁ into A₂. *Curr. Biol.* **25**, 3048–3057.

704

706 **Escobar-Camacho, D., Pierotti, M. E. R., Ferenc, V., Sharpe, D. M. T., Ramos, E., Martins, C. and Carleton, K. L.** (2019). Variable vision in variable environments: the visual system of an invasive cichlid (*Cichla monoculus*) in Lake Gatun, Panama. *J. Exp. Biol.* **222**,.

708

710 **Fox, J. and Weisberg, S.** (2018). *An R Companion to Applied Regression*. SAGE Publications.

712 **Frau, S., Loentgen, G., Martín-Robles, Á. J. and Muñoz-Cueto, J. A.** (2020). Ontogenetic expression rhythms of visual opsins in senegalese sole are modulated by photoperiod and light spectrum. *J. Comp. Physiol. B* **190**, 185–204.

714 **Fuller, R. C. and Claricoates, K. M.** (2011). Rapid light-induced shifts in opsin expression: finding new opsins, discerning mechanisms of change, and implications for visual sensitivity. *Mol. Ecol.* **20**, 3321–3335.

716 **Fuller, R. C., Carleton, K. L., Fadool, J. M., Spady, T. C. and Travis, J.** (2005). Genetic and environmental variation in the visual properties of bluefin killifish, *Lucania goodei*. *J. Evol. Biol.* **18**, 516–523.

718

720 **Goswami, U. C. and Barua, A. B.** (1981). Distribution of retinol & dehydroretinol in freshwater fish. *Indian J. Biochem. Biophys.* **18**, 383–385.

722 **Grabherr, M. G., Haas, B. J., Yassour, M., Levin, J. Z., Thompson, D. A., Amit, I., Adiconis, X., Fan, L., Raychowdhury, R., Zeng, Q., et al.** (2011). Full-length transcriptome assembly from RNA-Seq data without a reference genome. *Nat. Biotechnol.* **29**, 644–652.

724

726 **Halstenberg, S., Lindgren, K. M., Samagh, S. P., Nadal-Vicens, M., Balt, S. and Fernald, R. D.** (2005). Diurnal rhythm of cone opsin expression in the teleost fish *Haplochromis burtoni*. *Vis. Neurosci.* **22**, 135–141.

728 **Härer, A., Torres-Dowdall, J. and Meyer, A.** (2017). Rapid adaptation to a novel light environment: The importance of ontogeny and phenotypic plasticity in shaping the visual system of Nicaraguan Midas cichlid fish (*Amphilophus citrinellus* spp.). *Mol. Ecol.* **26**, 5582–5593.

730

732 **Härer, A., Meyer, A. and Torres-Dowdall, J.** (2018). Convergent phenotypic evolution of the visual system via different molecular routes: How Neotropical cichlid fishes adapt to novel light environments. *Evolution Letters* 1–14.

734

736 **Hofmann, C. M., O'Quin, K. E., Smith, A. R. and Carleton, K. L.** (2010). Plasticity of opsin
gene expression in cichlids from Lake Malawi. *Mol. Ecol.* **19**, 2064–2074.

738 **Kane, M. A. and Napoli, J. L.** (2010). Quantification of endogenous retinoids. *Methods Mol. Biol.* **652**, 1–54.

740 **Karagic, N., Härer, A., Meyer, A. and Torres-Dowdall, J.** (2018). Heterochronic opsin
expression due to early light deprivation results in drastically shifted visual sensitivity in a
cichlid fish: Possible role of thyroid hormone signaling. *J. Exp. Zool. B Mol. Dev. Evol.*
742 **330**, 202–214.

744 **Karagic, N., Härer, A., Meyer, A. and Torres-Dowdall, J.** (2022). Thyroid hormone tinkering
elicits integrated phenotypic changes potentially explaining rapid adaptation of color
vision in cichlid fish. *Evolution* **76**, 837–845.

746 **Krueger, F.** (2019). *Trim Galore! [Online]*.

748 **Landers, G. M. and Olson, J. A.** (1988). Rapid, simultaneous determination of isomers of
retinal, retinal oxime and retinol by high-performance liquid chromatography. *J. Chromatogr.* **438**, 383–392.

750 **Lenth, R., Singmann, H., Love, J., Buerkner, P. and Herve, M.** (2019). emmeans: Estimated
marginal means, aka least-squares means (R package version 1.1)[Computer software].

752 **Liebman, P. A. and Entine, G.** (1968). Visual pigments of frog and tadpole (*Rana pipiens*).
Vision Res. **8**, 761–775.

754 **Lythgoe, J. N.** (1980). *The ecology of vision*. Oxford: Clarendon Press.

756 **Lythgoe, J. N.** (1988). Light and Vision in the Aquatic Environment. In *Sensory Biology of
Aquatic Animals*, pp. 57–82. Springer New York.

758 **Maia, R., Gruson, H., Endler, J. A. and White, T. E.** (2019). pavo 2: New tools for the spectral
and spatial analysis of colour in r. *Methods in Ecology and Evolution* **64**, 1097–1107.

760 **Makino, M., Nagai, K. and Suzuki, T.** (1983). Seasonal variation of the vitamin A2-based visual
pigment in the retina of adult bullfrog, *Rana catesbeiana*. *Vision Res.* **23**, 199–204.

762 **Mapping the potential distribution of the invasive Red Shiner, Cyprinella lutrensis
(Teleostei: Cyprinidae) across waterways of the conterminous United States.**

764 **Margetts, B. M., Stuart-Fox, D. and Franklin, A. M.** (2024). Red vision in animals is broadly
associated with lighting environment but not types of visual task. *Ecol. Evol.* **14**, e10899.

766 **Marshall, J., Carleton, K. L. and Cronin, T.** (2015). Colour vision in marine organisms. *Curr.
Opin. Neurobiol.* **34**, 86–94.

768 **Matthews, W. J.** (1986). Geographic variation in thermal tolerance of a widespread minnow
Notropis lutrensis of the North American mid-west. *J. Fish Biol.* **28**, 407–417.

770 **Matthews, W. J. and Hill, L. G.** (1977). Tolerance of the Red Shiner, *Notropis lutrensis*
(Cyprinidae) to Environmental Parameters. *Southwest. Nat.* **22**, 89–98.

772 **McFarland, W. N. and Allen, D. M.** (1977). The effect of extrinsic factors on two distinctive
rhodopsin-porphropsin systems. *Can. J. Zool.* **55**, 1000–1009.

774 **Melsted, P., Ntranos, V. and Pachter, L.** (2019). The barcode, UMI, set format and BUStools.
Bioinformatics **35**, 4472–4473.

776 **Morshedian, A., Toomey, M. B., Pollock, G. E., Frederiksen, R., Enright, J. M., McCormick,
S. D., Cornwall, M. C., Fain, G. L. and Corbo, J. C.** (2017). Cambrian origin of the
CYP27C1-mediated vitamin A1-to-A2 switch, a key mechanism of vertebrate sensory
plasticity. *R Soc Open Sci* **4**, 170362.

780 **Muntz, W. R. and Mouat, G. S.** (1984). Annual variations in the visual pigments of brown trout
inhibiting lochs providing different light environments. *Vision Res.* **24**, 1575–1580.

782 **Munz, F. W. and Schwanzara, S. A.** (1967). A nomogram for retinene-2-based visual
pigments. *Vision Res.* **7**, 111–120.

784 **Musilova, Z. and Cortesi, F.** (2023). The evolution of the green-light-sensitive visual opsin
genes (RH2) in teleost fishes. *Vision Res.* **206**, 108204.

786 **Nandamuri, S. P., Yourick, M. R. and Carleton, K. L.** (2017). Adult plasticity in African
cichlids: Rapid changes in opsin expression in response to environmental light
differences. *Mol. Ecol.* **26**, 6036–6052.

788 **Papatheodorou, I., Fonseca, N. A., Keays, M., Tang, Y. A., Barrera, E., Bazant, W., Burke,
M., Füllgrabe, A., Fuentes, A. M.-P., George, N., et al.** (2018). Expression Atlas: gene
and protein expression across multiple studies and organisms. *Nucleic Acids Res.* **46**,
D246–D251.

792 **Pimentel, H., Bray, N. L., Puente, S., Melsted, P. and Pachter, L.** (2017). Differential analysis
of RNA-seq incorporating quantification uncertainty. *Nat. Methods* **14**, 687–690.

794 **Rennison, D. J., Owens, G. L., Heckman, N., Schluter, D. and Veen, T.** (2016). Rapid
adaptive evolution of colour vision in the threespine stickleback radiation. *Proc. Biol. Sci.*
283, 20160242.

798 **Ricci, V., Ronco, F., Boileau, N. and Salzburger, W.** (2023). Visual opsin gene expression
evolution in the adaptive radiation of cichlid fishes of Lake Tanganyika. *Sci Adv* **9**,
eadg6568.

800 **Seehausen, O., Terai, Y., Magalhaes, I. S., Carleton, K. L., Mrosso, H. D. J., Miyagi, R., van
der Sluijs, I., Schneider, M. V., Maan, M. E., Tachida, H., et al.** (2008). Speciation
through sensory drive in cichlid fish. *Nature* **455**, 620–626.

804 **Smithson, M. and Verkuilen, J.** (2006). A better lemon squeezer? Maximum-likelihood
regression with beta-distributed dependent variables. *Psychol. Methods* **11**, 54–71.

806 **Team, R. C.** (2021). R: A language and environment for statistical computing. Published online
2020.

808 **Temple, S. E., Plate, E. M., Ramsden, S., Haimberger, T. J., Roth, W. M. and Hawryshyn, C. W.** (2006). Seasonal cycle in vitamin A₁/A₂-based visual pigment composition during the life history of coho salmon (*Oncorhynchus kisutch*). *J. Comp. Physiol. A Neuroethol. Sens. Neural Behav. Physiol.* **192**, 301–313.

810

812 **Terai, Y., Miyagi, R., Aibara, M., Mizoiri, S., Imai, H., Okitsu, T., Wada, A., Takahashi-Kariyazono, S., Sato, A., Tichy, H., et al.** (2017). Visual adaptation in Lake Victoria cichlid fishes: depth-related variation of color and scotopic opsins in species from sand/mud bottoms. *BMC Evol. Biol.* **17**, 200.

814

816 **Tsin, A. T. C. and Beatty, D. D.** (1977). Visual Pigment Changes in Rainbow Trout in Response to Temperature. *Science* **195**, 1358–1360.

818

820 **Ueno, Y., Ohba, H., Yamazaki, Y., Tokunaga, F., Narita, K. and Hariyama, T.** (2005). Seasonal variation of chromophore composition in the eye of the Japanese dace, *Tribolodon hakonensis*. *J. Comp. Physiol. A Neuroethol. Sens. Neural Behav. Physiol.* **191**, 1137–1142.

822 **Veen, T., Brock, C., Rennison, D. and Bolnick, D.** (2017). Plasticity contributes to a fine-scale depth gradient in sticklebacks' visual system. *Mol. Ecol.* **26**, 4339–4350.

824 **Wald, G.** (1957). The metamorphosis of visual systems in the sea lamprey. *J. Gen. Physiol.* **40**, 901–914.

826 **Whitmore, A. V. and Bowmaker, J. K.** (1989). Seasonal variation in cone sensitivity and short-wave absorbing visual pigments in the rudd *Scardinius erythrophthalmus*. *J. Comp. Physiol. A Neuroethol. Sens. Neural Behav. Physiol.* **166**, 103–115.

828 **Wickham, H., Averick, M., Bryan, J., Chang, W., McGowan, L. D., François, R., Grolemund, G., Hayes, A., Henry, L., Hester, J., et al.** (2019). Welcome to the tidyverse. *Journal of Open Source Software* **4**, 1686.

830

832 **Wilwert, E., Etienne, R. S., van de Zande, L. and Maan, M. E.** (2022). Contribution of opsins and chromophores to cone pigment variation across populations of Lake Victoria cichlids. *J. Fish Biol.* **101**, 365–377.

834 **Wilwert, E., Etienne, R. S., van de Zande, L. and Maan, M. E.** (2023). Visual system plasticity is differently mediated by cone opsin expression and chromophore composition in closely related cichlid species. *Hydrobiologia* **850**, 2299–2314.

836

838 **Zonta, F. and Stancher, B.** (1984). High-performance liquid chromatography of retinols, retinols (vitamin A₁) and their dehydro homologues (vitamin A₂): improvements in resolution and spectroscopic characterization of the stereoisomers. *J. Chromatogr.* **301**, 65–75.

840

842 Figure Legends:

Figure 1. The light environments of our study sites differ in turbidity,

844 **transmittance, and spectral composition.** (a) Representative images of our study
sites: Lighting Creek (left), Big Creek (middle), and Polecat Creek (right, photo: Meridian
846 Engineering). (b) Turbidity of each site measured in Nephelometric Turbidity Units
(NTU) for the years spanning from 2011-2018. The bar indicates the mean turbidity in
848 each site and season. Turbidity data provided courtesy of the Oklahoma Conservation
Commission. (c) The transmittance measured as the total irradiance 350-700 nm
850 wavelength at 20 cm depth divided by total irradiance at the water's surface. The bar
indicates the mean irradiance at each site and season. (d) The spectral composition of
852 light at 20 cm depth measured as the ratio of red irradiance (550-650 nm) to blue
irradiance (350-450 nm). The bar indicates the mean red:blue ratio at each site in each
854 season.

Figure 2. The chromophore composition of the red shiner eye differs among sites

856 **and with seasons and is correlated with eye size.** (a) Proportion of A₂ chromophore
relative to total retinoid content of whole eyes. Each point represents an individual and
858 the bar represents the mean proportion of A₂ chromophore at each site in each season.
(b) Proportion of A₂ chromophore relative to eye diameter. Each point represents an
860 individual and the line is a simple linear regression fit to the data from each site.

Figure 3. Red shiner CYP27C1 converts retinol to 3,4-didehydroretinol. (a) HPLC-

862 DAD profiles of retinoids extracted from HEK293 cells transfected with a control
construct (black) or red shiner CYP27C1 expression vector (red). (b) UV-Vis
864 absorbance spectra of the retinol substrate (peak 1) and the novel product of CYP27C1
(peak 2). The retention time and UV-Vis spectrum of peak 2 is consistent with 3,4-
866 didehydroretinol.

Figure 4. Opsin and CYP27C1 expression. (a) Normalized gene expression

868 measured as transcripts per million (TPM) for individual samples at a clear water site
(Lightning Creek) or turbid water site (Polecat Creek). Each point represents an
870 individual and bars indicate mean expression at each site in each season. (b) The

expression of each opsin gene relative to total opsin expression with an individual eye.

872 Each point represents an individual and bars indicate mean relative expression at each site in each season.

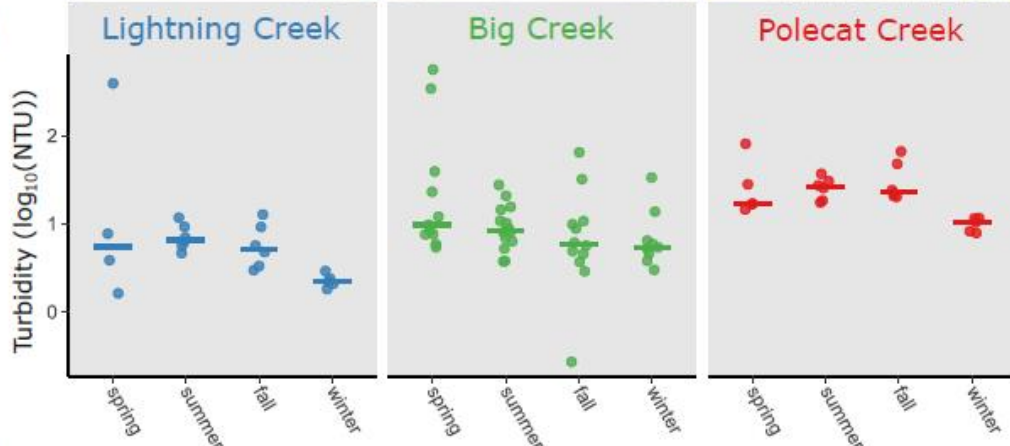
874

Figure 1.

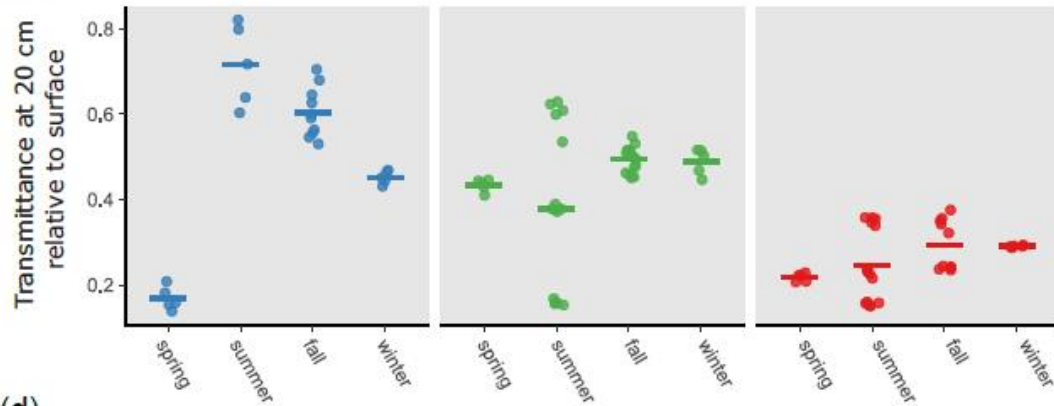
(a)



(b)



(c)



(d)

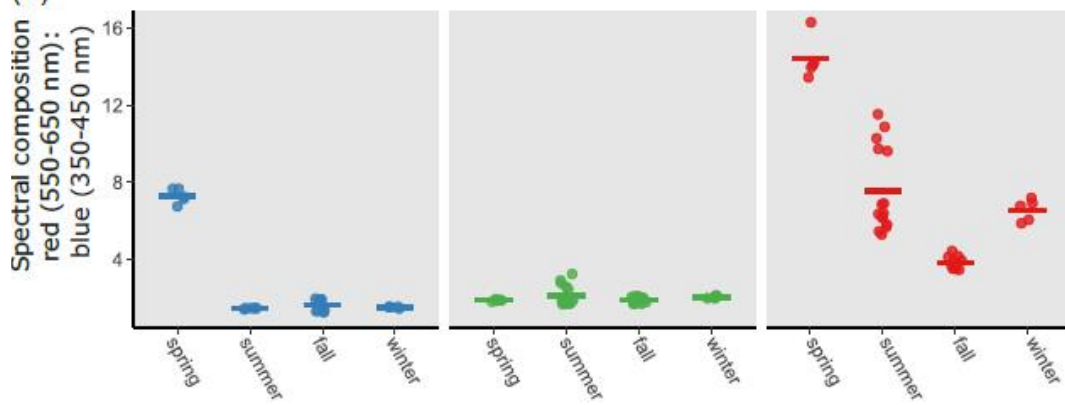
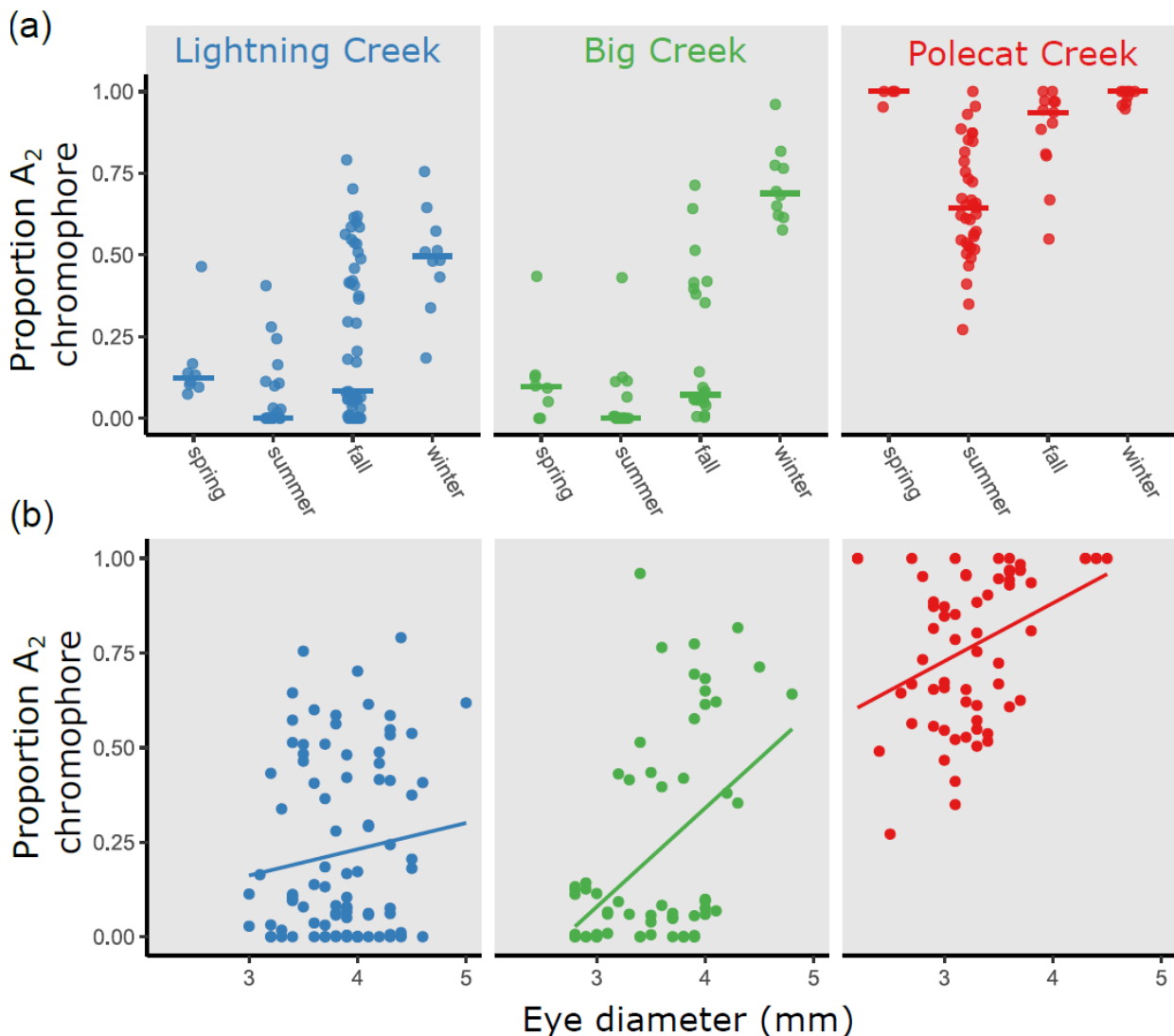
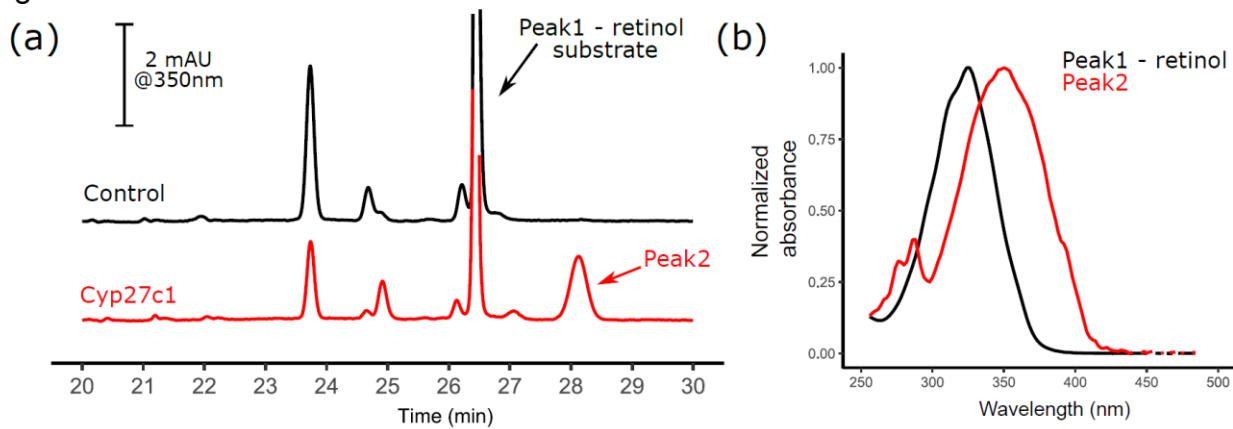


Figure 2.



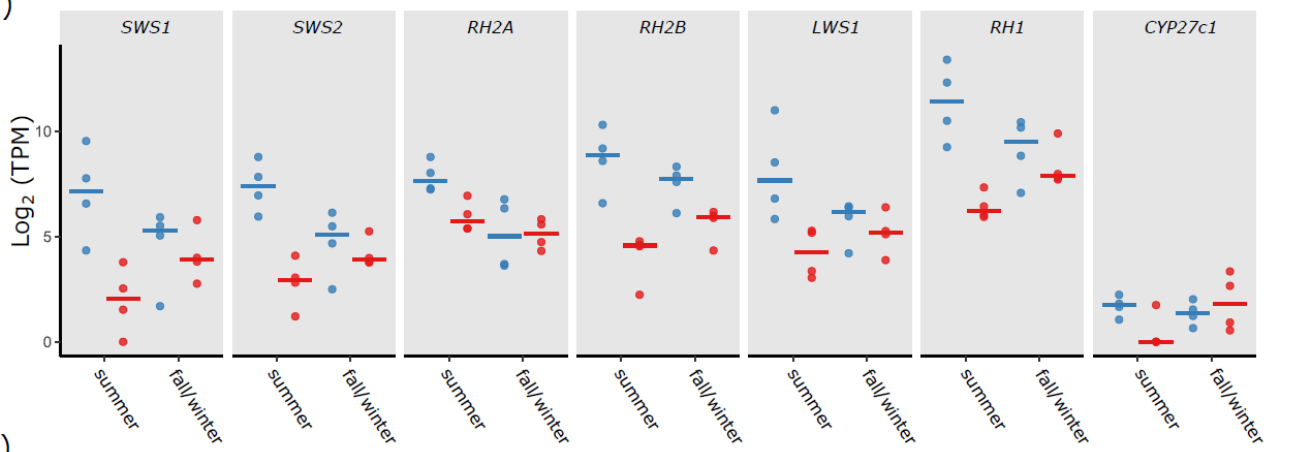
880 Figure 3.



882

Figure 4.

(a)



(b)

